

Maris polarization in neutron-rich nuclei

Shubhchintak

Department of Physics, Texas A&M University-Commerce, Commerce, TX 75924, USA

C.A. Bertulani

*Department of Physics and Astronomy, Texas A&M University-Commerce, Commerce, TX 75429-3011, USA and
Institut für Kernphysik, Technische Universität Darmstadt, D-64289 Darmstadt, Germany*

T. Aumann

*Institut für Kernphysik, Technische Universität Darmstadt, D-64289 Darmstadt, Germany and
GSI Helmholtzzentrum für Schwerionenforschung, Planckstr. 1, 64291 Darmstadt, Germany*

We study the application of Maris polarization to assess information on the evolution of neutron skins along a nuclear isotopic chain. First we discuss the uncertainties in the determination of triple differential cross sections and of analyzing powers on the nucleon-nucleon interaction, optical potentials, and medium effects. A method is devised to extract information on neutron skins from asymmetries due to Maris polarization on the analyzing power measurements. Limitations of the method are discussed. We show that the neutron skin amplifies the magnitude of the Maris polarization effect which can be used as an effective way of checking the absorption effect included in reaction theories.

The spin-orbit interaction is one of the most celebrated findings in our quest to understand the nature of nuclei. In 1936, Inglis [1] investigated the microscopic origin of the nuclear spin-orbit interaction by adding to nuclear forces a copycat of the atomic spin-orbit coupling, also known as the relativistic Thomas effect [2]. Years later, the phenomenological inclusion of the spin-orbit interaction in the nuclear shell model, together with the Pauli principle, allowed an astonishingly simple explanation of the magic numbers appearing in nuclear energy spectra. The interaction was assumed to be much larger than the relativistic effect proposed by Inglis. This achievement had a large impact in our understanding of nuclear systems and led to a Nobel prize for Mayer and Jensen in 1950 [3, 4]. The microscopic origins of the nucleon-nucleus spin-orbit force are now explained in terms of a quantum field description of σ and ω meson exchange [5].

The spin-orbit interaction is of fundamental importance to explain basic phenomena observed in atomic and nuclear collisions. In nuclear physics, the simplest of all collisional cases, namely, elastic collision differential cross sections, display interference of polarized protons scattering through the near side and the far side of the nucleus. This interference pattern can be explained in terms of the opposite signs of the $\mathbf{s} \cdot \mathbf{L}$ spin-orbit term due to the angular momentum flip (see, e.g., Ref. [6]) in changing from the near to the far side. Evidently, other types of direct collisions using polarized protons are also influenced by the strength of the spin-orbit force and serve as a probe of its modification in the nuclear medium. For example, one has speculated modifications of nucleon and meson masses and sizes, and also of meson-nucleon coupling constants in nuclear medium, motivated by strong relativistic nuclear fields in the medium, deconfinement of quarks, and also partial chiral symmetry restoration [14–18]. A density dependence of the nucleon-nucleon interaction is obviously expected, modifying the expect-

tations for nucleon induced reactions based on bare interactions.

With the availability of high-energy radioactive beams, quasifree (p,2p) and (p,pn) reactions have again become a standard experimental tool to study nuclear spectroscopy. Newly developed detectors have allowed efficient experiments using inverse kinematics with hydrogen targets and opened new possibilities to investigate the single-particle structure and nucleon-nucleon correlations as the neutron-to-proton ratio of secondary beam projectiles increases. Such new developments are possible due to the detection of all outgoing particles, providing kinematically complete measurements of the reactions carried out at the GSI/Germany, RIKEN/Japan, and other nuclear physics facilities. First experiments using (p,2p) and (p,pn) with newly developed experimental techniques have already been reported with success [7–10]. These experiments have focused on the reliability of quasi-free scattering using inverse kinematics as a technique to study the shell-evolution in neutron-rich nuclei. Problems such as quenching of spectroscopy factors and single-particle properties of neutron-rich nuclei have been studied. Recent theoretical work on (p,2p) reactions have also been reported [8, 11–13].

In this article, we explore the extension of quasi-free scattering of radioactive beams on polarized proton targets. In particular, we will focus on the role of the spin-orbit interaction as a means to investigate neutron skins in nuclei and the density dependence of the nucleon-nucleon interaction in asymmetric nuclear matter. We show that the effective polarization of knocked out protons increase steadily with the neutron number, a clear indication of the mean radius increase of the nuclei due to a pile-up of neutrons at its surface. The induced polarization due to a combination of absorption and spin is known as the “Maris effect” [19–21]. The idea is rather simple and invokes a combination of absorption and spin-

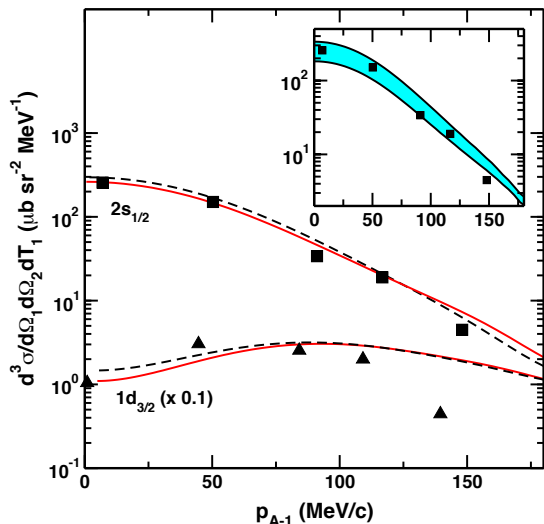


Figure 1: (Color online) Cross sections for $^{40}\text{Ca}(p,2p)^{39}\text{K}$ and $E_p = 148$ MeV, as a function of the recoil momentum, p_{A-1} of the the residual nucleus. The proton knockout are assumed to be from the $1d_{3/2}$ and $2s_{1/2}$ orbitals in ^{40}Ca . The cross sections are integrated over the energy of knocked-out proton and given in units of $\mu\text{b sr}^{-2} \text{MeV}^{-1}$. The experimental data is from Ref. [28]. In the big panel the dashed (solid) lines include (do not) the spin-orbit interaction. The inset shows the modification of the calculation for the $1s_{1/2}$ state with the inclusion of several NN-interactions. The shaded lines include a broad range of results obtained with the different NN-interactions.

orbit interaction. Suppose that the primary polarized proton is detected on the large-angle side of the momentum transfer q . Proton initial momenta directed toward the large-angle side of q , correspond to spin-up protons with $j = l - 1/2$ on the near side and to $j = l + 1/2$ on the far side. Initially polarized nucleons knocked out from the near side will undergo less attenuation on their way out than those from the far side. Therefore they are less polarized, $P_N < 0$, for $j = l - 1/2$. The reverse is true, and $P_N > 0$, for $j = l + 1/2$. The resulting net polarization of the knocked out nucleons when summed over their subshells would vanish for a closed-shell nucleus if the subshell momentum distributions were identical and if the NN interaction were spin-independent. But they are not and will cause differences in $P_N^{(near)}$ and $P_N^{(far)}$. Therefore, one expect that due to absorption and the spin-orbit part of the optical potential, Maris polarization is approximately twice as large for $1p_{1/2}$ as for $1p_{3/2}$ and also opposite in sign. The net polarization of the knocked-out nucleon can be observed using polarized proton targets and exploiting the difference between the (spin-up)-(spin-up) and (spin-down)-(spin-up) cross sections in triplet and singlet scattering, respectively [19–21].

(p,2p) reactions are thought to be simpler than the

elastic nuclear scattering mentioned above. This statement is based on the argument that in elastic scattering one deals with the scattering amplitudes of all nucleons in the nucleus, whereas (p,2p) reactions involves the scattering amplitude of a single nucleon in the nucleus. Absorption in this case is used as a benefit to enhance the effective polarization.

Polarized protons can also be used to probe the density dependence of the nucleon-nucleon (NN) interaction. A reduction of the analyzing power, A_y , due to density dependence has indeed been discussed in Refs. [18, 22]. An approximate 40% reduction of A_y has been predicted in the case of the $^{12}\text{C}(p,2p)$ reaction, where the averaged density within ^{12}C is about 50% of the saturation density. In Ref. [23] it was also suggested that the reduction of meson masses and coupling constants in dense nuclear matter will cause modifications of spin observables in quasifree reactions, explaining why the A_y are reduced by about 40% when the matter density is about 50% of the saturation density. These expectations have been verified experimentally [24].

Before we assess the importance of Maris polarization to probe asymmetric nuclear matter using neutron-rich projectiles, we discuss how well existing experimental data can be understood with our calculations based on a standard theory of quasifree reactions. The triple differential cross sections for quasifree scattering in the Distorted Wave Impulse Approximation (DWIA) is given by [25]

$$\frac{d^3\sigma}{d\Omega_1 d\Omega_2 dT_1} = C^2 S \cdot K_F \times \left| \left\langle \chi_{\sigma_2 \mathbf{k}_{p_2}}^{(-)} \chi_{\sigma_1 \mathbf{k}_1}^{(-)} | \tau_{pN} | \chi_{\sigma_0 \mathbf{k}_0}^{(+)} \psi_{jlm} \right\rangle \right|^2, \quad (1)$$

where K_F is a kinematic factor, p_0 (p_1) denotes the incoming (outgoing) proton, p_2 the knocked-out nucleon, T_2 its energy, $C^2 S$ is the spectroscopic factor associated with the single-particle properties of p_2 in the nucleus and ψ_{jlm} is the nucleon wavefunction, which in the naïve single-particle model is labelled by the jlm quantum numbers. The DWIA matrix element includes the scattering waves for the incoming and outgoing nucleons, with information on their spins and momenta, $(\sigma \mathbf{k})$, as well and the t-matrix for the nucleon-nucleon scattering. To first-order this t-matrix is directly proportional to the NN interaction. For unpolarized protons, Eq. (1) has to be averaged over initial spin orientations besides a sum over final spin orientations. This formalism has been used previously in several calculations and a good description of experimental data has been achieved with proper choices of optical potential and the nucleon-nucleon interaction (see, e.g., Refs. [26, 27]). In Ref. [7] it was shown that momentum distributions of the residual nuclei obtained in quasi-free scattering are well described using the eikonal approximation for the scattering waves $\chi_{\mathbf{k}_i}$ entering Eq. (1). The eikonal waves allow one to include relativistic and medium effects easily and a connection with partial waves can be done for large angular

momenta with $L = kb$, where k is the bombarding momentum and b the impact parameter. In order to keep track of the Maris effect for any angular momentum, we adopt here the partial wave method used in most previous theoretical works [19–27].

In Figure 1 we show the cross sections for $^{40}\text{Ca}(p,2p)^{39}\text{K}$ and $E_p = 148$ MeV, as a function of the recoil momentum, p_{A-1} of the the residual nucleus. The proton knockout is assumed to be from the $1d_{3/2}$ and $2s_{1/2}$ orbitals in ^{40}Ca . The cross sections are integrated over the energy of knocked-out proton and given in units of $\mu\text{b sr}^{-2} \text{MeV}^{-1}$. The experimental data is from Ref. [28]. In the big panel the dashed (solid) lines include (do not) the spin-orbit interaction. The optical potential of Ref. [29] was used together with NN-interaction from Ref. [30]. In agreement with the conclusions of Refs. [28, 31], we find that the spin-orbit effect is rather small for unpolarized protons. The inset shows the comparison with the experimental data for the $1s_{1/2}$ state as the NN-interaction is changed. The shaded area includes results for seven NN-interactions taken from Refs. [30, 32–37]. It is clear that the proper choice of the interaction has a greater impact on the results for unpolarized protons than the spin-orbit interaction. The same conclusion applies for the proton removal from the $1d_{3/2}$ orbital. Not shown for simplicity are sources of uncertainty in the numerical results arising with the adoption of different global optical potentials. They also yield a broad range of results, as with the case of the NN interactions.

We now turn to the effects of the density dependence on the cross sections and analyzing power,

$$A_y = \frac{d\sigma(\uparrow) - d\sigma(\downarrow)}{d\sigma(\uparrow) + d\sigma(\downarrow)}, \quad (2)$$

which requires the detection of knocked out nucleons by incoming polarized protons with opposite polarizations. To describe the analyzing power one needs to properly account for the spin variables in the transition matrix of Eq. (1). This procedure has been described in details in Refs. [19–27]. The density dependence of the interaction has been assumed to be of the form proposed in Ref. [22], namely, one assumes that the NN t-matrix is modified because the nucleon mass in the nuclear medium, $m^*(r)$ changes locally according to

$$m_N^*(r) = \left[1 - 0.44 \frac{\rho(r)}{\rho_0} \right] m_N, \quad (3)$$

where $\rho(r)$ is the density at radius r , ρ_0 is the nuclear saturation density of 0.17 fm^{-3} , and the factor -0.44 stems from the relativistic mean field theory [18]. This effect is obtained from a Schrödinger equivalent form of the Dirac description of the scattering waves χ_i . The spinor parts of these waves are then incorporated into the NN t-matrix, with the nucleon mass replaced by m_N^* within the nucleon spinors [22]. This effect is somewhat reminiscent of the modification of meson masses and coupling constant in the Rho-Brown scaling conjecture [15] so that

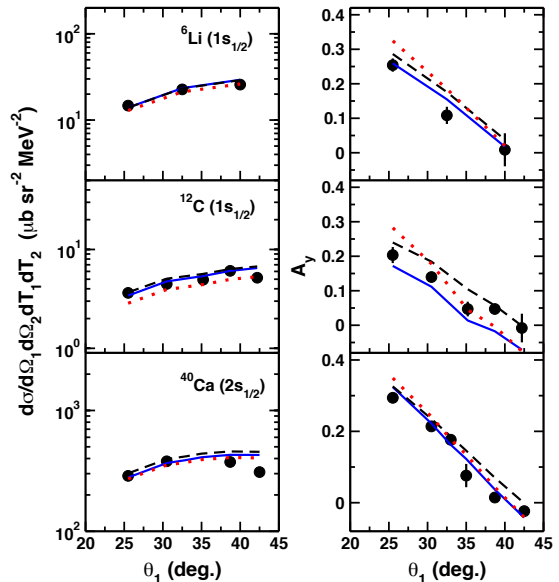


Figure 2: (Color online) Cross sections and analyzing powers for (p,2p) reactions on ^6Li , ^{12}C and ^{40}Ca at 392 MeV. The solid lines include the spin-orbit part of the optical potential, the dashed lines display the results without the spin-orbit part, and the dotted-lines contain spin-orbit but neglect the density dependence in the NN t-matrix. The data are from Ref. [24].

the masses of the mesons giving rise to the interaction are modified according to $m_{\sigma}^*/m_{\sigma} = m_{\rho}^*/m_{\rho} = m_{\omega}^*/m_{\omega} = \xi$ and $g_{\sigma N}^*/g_{\sigma N} = g_{\omega N}^*/g_{\omega N} = \chi$. It has been applied previously in Ref. [23] to study nuclear medium effects in quasi-free scattering, with the parameters ξ and χ varying within the range $0.6 - 0.9$.

In Figure 2 we present our results for (p,2p) reactions on ^6Li , ^{12}C and ^{40}Ca at 392 MeV, based on Eq. (3) in the model proposed by Horowitz and Iqbal [22]. The data are from Ref. [24]. Here we use the NN interaction from Ref. [38] and the Dirac phenomenological optical potential from Ref. [39], where the inclusion of the modification in Eq. (3) is straightforward. The solid lines include the spin-orbit part of the optical potential and the calculations have been normalized to the data for $d^3\sigma/d\Omega_1 d\Omega_2 dT_1$. Due to the nature of the data analysis [24], we do not try to identify them as spectroscopic factors which are also irrelevant for the calculation of A_y . The dashed lines display the results without the spin-orbit part, and the dotted-lines contain spin-orbit but neglect the density dependence in the NN t-matrix. The usage of s-shell protons is chosen because the interpretation is rather simplified since Maris polarization (discussed below) should be small, although the knocked out nucleon can still acquire a non-zero angular momentum with respect to the (A-1) residue after the collision. In fact, the target protons are unpolarized and the scattering asymmetry should be nearly equal to the asymmetry

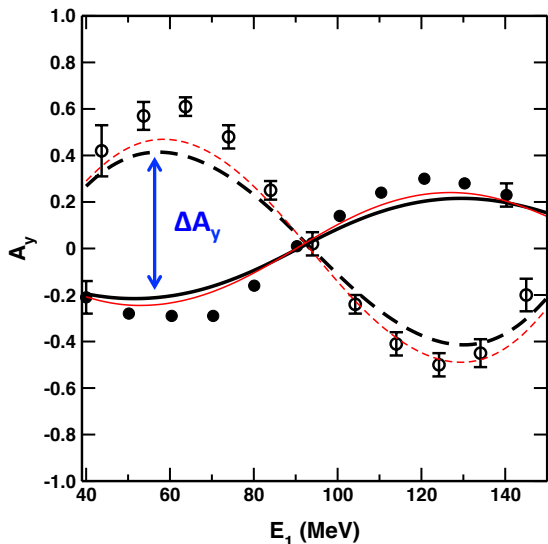


Figure 3: (Color online) Analyzing powers for the $1p_{3/2}$ and $1p_{1/2}$ states in $^{16}\text{O}(p,2p)$ reaction at 200 MeV as a function of the kinetic energy of the ejected proton. Thin (thicker) lines include (do not include) the medium modification of the NN interaction. One proton is measured at 30° and the other at -30° . The open circles are for $1p_{1/2}$ and the solid circles for $1p_{3/2}$. The thinner (thicker) lines include (do not include) the medium modification of the NN interaction.

for the scattering of free protons. But we observe that the spin-orbit effect still plays a role even for nucleons knocked from s-waves because of the non-negligible angular momentum transfer in the collision.

Maris polarization is a combined action of absorption and spin-orbit force for a nucleon knocked out a non-zero angular momentum orbital, such as $p_{1/2}$ and $p_{3/2}$ nucleons. The ejected nucleon is polarized before the collision and an average over the spin tends to wash out this polarization, except that the interaction with the incoming polarized proton has a strong spin dependence. This leads to a net effective polarization which depends on the sub-shell where the nucleon is ejected from. But, as shown in Ref. [21], the effective polarization is not far from being proportional to A_y . Therefore, Maris polarization is also directly visible in analyzing power data. This is best seen if A_y is displayed for fixed angles of the outgoing nucleons and scanning the energy of the ejected nucleon, as seen in Figure 3. The data are from Ref. [40]. Both nucleons are measured at 30° . The open circles are for $1p_{1/2}$ and the solid ones for $1p_{3/2}$. Thinner (thicker) lines include (do not include) the medium modification of the NN interaction. Here and in the following we use the same NN interaction and optical potential model as in the calculations of Fig. 1.

As the number of neutrons increase in an isotopic chain, the isotope develops a neutron skin. While the charge distribution in stable nuclei is well determined via electron scattering experiments, similar experiments

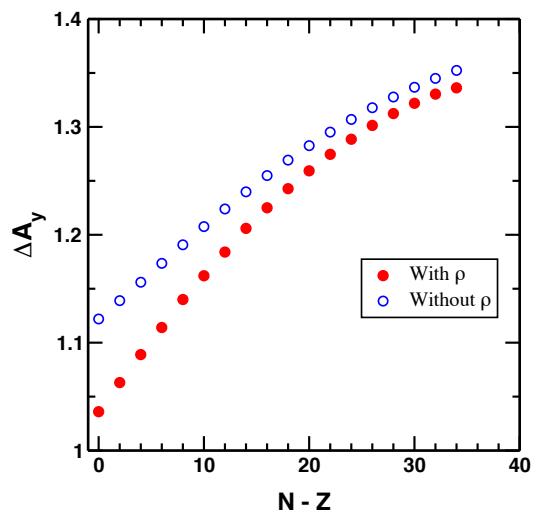


Figure 4: (Color online) Difference in the polarization maximum and minimum for the $2p_{1/2}$ and $2p_{3/2}$ subshells in tin isotopes for (p,2p) reactions at 200 MeV as a function of the neutron excess. The solid (open) circles include (do not include) density dependence of the NN interaction. We assume that protons are detected at $\theta = 35^\circ$ and $\theta = -35^\circ$, respectively.

done on unstable nuclei are very difficult. Projects along these lines have been proposed but are still far from being realized [41–43]. Besides, the determination of neutron skin in a nucleus requires also measurements of the neutron (or matter) density separately. Efforts in this direction involve several experimental methods, such as measurement of interaction cross sections [44], parity violation in weak interaction with electron scattering [45], Coulomb dissociation [46], antiprotonic atoms [47], dipole polarization in (p,p') scattering [48], etc. The analyzing power, being a ratio of cross sections, factors out some of the uncertainties associated in the calculations, such as the magnitude of spectroscopic factors. Moreover, the Maris effect is more sensitive to the surface region of the nucleus than the triple differential cross sections.

We explore Maris polarization in neutron-rich nuclei and its dependence on the neutron number by studying the tin isotopic chain which is well described with standard mean field theories. We include the density dependence of the interaction according to the prescription in Eq. (3) with nuclear densities calculated with the Hartree-Fock-Bogoliubov (HFB) method and the BSk2 Skyrme interaction, as described in Ref. [49]. We need the single-particle energies as well as the wavefunction of the ejected nucleon. It is possible, but complicated and not necessarily reliable, to extract these quantities from the HFB mean field method. We adopt a simpler approach to determine these quantities from a global Woods-Saxon potential model in the form $V(r) = [V_0 + (0.72 \text{ fm}^2)V_{SO}/(ar)]f(r)$, $f(r) =$

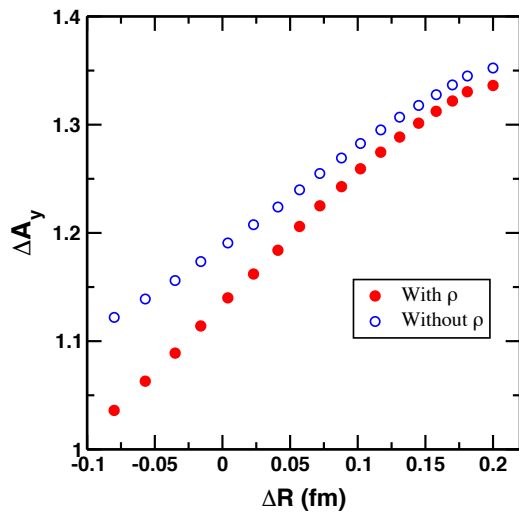


Figure 5: (Color online) Difference in the polarization maximum and minimum for the $2p_{1/2}$ and $2p_{3/2}$ subshells in tin isotopes for (p,2p) reactions at 200 MeV as a function of the neutron skin. The solid (open) circles include (do not include) density dependence of the NN interaction. We assume that protons are detected at $\theta = 35^\circ$ and $\theta = -35^\circ$, respectively.

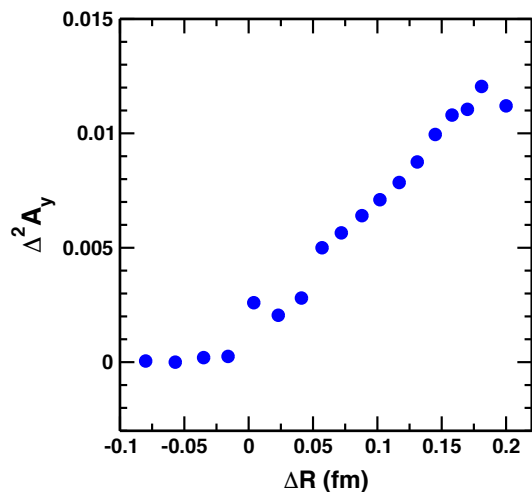


Figure 6: (Color online) A higher order quantification of the Maris polarization to extract the neutron skin in tin isotopes. See text for more details.

$\{1 + \exp[(r - R)/a]\}^{-1}$, $V_0 = [-57.8 \pm 33(N - Z)/A]$ MeV with $+$ ($-$) sign for neutrons (protons), and $V_{SO} = [-22 \pm 14(N - Z)/A]$ MeV. We use $a = 0.65$ fm and $R = 1.2A^{1/3}$ fm. We assume that the protons are ejected from the $2p_{1/2}$ and $2p_{3/2}$ states.

The calculated analyzing powers for the tin isotopes have a similar feature as that displayed in Fig. 3. The magnitude of the Maris polarization will be quantified in terms of the difference between the first maximum of the $2p_{1/2}$ state and the first minimum of the $2p_{3/2}$ state,

denoted by

$$\Delta A_y = (A_y^{p_{1/2}})_{max} - (A_y^{p_{3/2}})_{min}. \quad (4)$$

In Figure 4 we plot ΔA_y in tin isotopes for (p,2p) reactions at 200 MeV as a function of the neutron excess. We assume that protons are detected at $\theta = 35^\circ$ and $\theta = -35^\circ$, respectively. The solid (open) circles include (do not include) the density dependence of the NN interaction. The same result is shown in Figure 5 as a function of the neutron skin $\Delta R = \langle r^2 \rangle_n^{1/2} - \langle r^2 \rangle_p^{1/2}$ obtained from the calculated rms radii for the HFB neutron and proton densities. It is evident that adding more neutrons to the system increases the magnitude of the Maris polarization. The effective polarization increases by more than 30% along the isotopic chain. The dependence with the neutron skin is almost linear, although deviations from the linear behavior appears at large neutron numbers. The inclusion of the density dependence of the NN interaction decreases ΔA_y for small neutron numbers and small skins. This difference is stronger for isospin symmetric nuclei than for asymmetric ones.

Since the proton radius is nearly constant along the isotopic chain, it is clear that the steady increase of ΔA_y is due to the build up of neutrons in the skin. However, one can also argue that this occurs simply because of the increase of absorption with the nuclear size either with symmetric or asymmetric isospin content. In this case, adding more neutrons to a nucleus would extend its matter distribution both for neutrons and for protons up to the same mean nuclear radius. In order to clarify this statement, we have calculated ΔA_y for proton (ΔA_y^p) and for neutron (ΔA_y^n) densities separately, whereby both densities are renormalized to the mass number A . By averaging these results and subtracting them from the previously calculated ΔA_y , i.e., by defining

$$\Delta^2 A_y = \Delta A_y - \frac{(\Delta A_y^n + \Delta A_y^p)}{2}, \quad (5)$$

we get an explicit dependence of the effect of the neutron skin, removing from it the bulk dependence on the matter radius. These results are shown in Figure 6. We still see an increase of the Maris polarization effect due to the build up of neutrons in the neutron skin but, as compared to the results presented in Figure 5, with the use of $\Delta^2 A_y$ the effect is now reduced by a factor 100. Nonetheless, the fact that A_y increases so firmly with the neutron number in neutron-rich nuclei can be used as a new and important determination of neutron skins in nuclei. As with the other known techniques, such as anti-protonic atoms, or electron scattering, it will increase the precision with which we can measure the nuclear matter radius as a function of the proton and neutron numbers.

In conclusion, we have investigated Maris polarization as a probe of the neutron skin growth along an isotopic chain. As the nuclear size increases, the asymmetric behavior in analyzing power measurements due to the combination of spin-orbit and absorption effects increase

accordingly. We have shown that the determination of neutron skins with such measurements can be done if a separate information on the nuclear charge density is known. An unequivocal determination of the neutron skin requires that the A_y measurements also explore the choices of nuclear interactions and account of medium effects. The choice of NN interactions, some of them also including medium modifications due to Pauli blocking and many-body effects, using e.g., a G-matrix approach, can be tested for a large number of experimental data already available.

The Maris polarization effect is an useful tool to investigate single-particle properties in nuclei and their evolution in neutron rich isotopes. Its sensitiveness to the strength of the spin-orbit interaction, medium modification of nucleon masses, and nuclear absorption allows for new applications in the studies carried out with secondary radioactive beams. Because experiments can now

be carried out with a much larger precision than in the past, new techniques are increasingly needed to extend our knowledge of the nuclear physics of neutron-rich nuclei. We have shown that the effective polarization of knocked out protons in (p,2p) reactions can be added to the new techniques to study the nuclear size measurements. indeed, the determination of neutron skins in nuclei is one of the major research efforts due to its relation to neutron stars and their equation of state [51].

This work was supported in part by the U.S. DOE grant DE-FG02-08ER41533 and the U.S. NSF Grant No. 1415656. We thank HIC for FAIR for supporting visits (C.A.B.) to the TU-Darmstadt. This project was also supported (T.A.) by the German Federal Ministry for Education and Research (BMBF project 05P15RDFN1), and through the GSI-TU Darmstadt cooperation agreement.

-
- [1] D.R. Inglis, Phys. Rev. 50, 783 (1936)
 [2] L.H. Thomas, Nature 117, 514 (1926).
 [3] M. Goeppert-Mayer, Phys. Rev. 78, 16 (1950)
 [4] O. Haxel, J.H.D. Jensen, and H.E. Suess, Z. Physik 128, 295 (1950).
 [5] R. Machleidt, “The Meson Theory of Nuclear Forces and Nuclear Structure”, Advances in Nuclear Physics 19, 189 (1989).
 [6] C.A. Bertulani and P. Danielewicz, “Introduction to Nuclear Reactions”, IOP Publishing (2004).
 [7] T. Aumann, Prog. Part. Nucl. Phys. 59, 3 (2007).
 [8] T. Aumann, C.A. Bertulani and J. Ryckebusch, Phys. Rev. C 88, 064610 (2013).
 [9] T. Kobayashi et al., Nucl. Phys. 805, 431c (2008).
 [10] V. Panin et al., Phys. Lett. B 753, 204 (2016).
 [11] Kazuyuki Ogata, Kazuki Yoshida, and Kosho Minomo, Phys. Rev. C 92, 034616 (2015).
 [12] A.M. Moro, Phys. Rev. C 92, 044605 (2015).
 [13] E. Cravo, R. Crespo and A. Deluva, Phys. Rev. C 93, 054612 (2016).
 [14] O.V. Miklukho et al., Phys. Atom. Nucl., 76, 871 (2013).
 [15] G.E. Brown and M. Rho, Phys. Lett. 66, 2720 (1991).
 [16] R.J. Furnstahl et al., Phys. Rev. C 46, 1507 (1992).
 [17] T. Hatsuda, Nucl. Phys. A 544, 27 (1992).
 [18] D. Serot and J.D. Walecka, in Advances in Nuclear Physics, Ed. by J.W. Negele and E. Vogt (Plenum Press, New York, 1986), Vol. 16, p. 116.
 [19] Th.A.J. Maris, Nucl. Phys. 9, 577 (1958/1959).
 [20] G. Jacob, Th.A.J. Maris, C. Schneider and M.R. Teodoro, Nucl. Phys. A257, 517 (1976).
 [21] Th.A.J. Maris, M.R. Teodoro and C.A.Z. Vasconcellos, Nucl. Phys. A 312, 461 (1979).
 [22] C.J. Horowitz and M.J. Iqbal, Phys. Rev. C 33, 2059 (1986).
 [23] G. Krein, Th.A.J. Maris, B.B. Rodrigues, and E. A. Veit, Phys. Rev. C 51, 2646 (1995).
 [24] K. Hatanaka et al., Phys. Rev. Lett. 78, 1014 (1997).
 [25] G. Jacob and Th.A.J. Maris, Rev. Mod. Phys. 38, 121 (1966); *ibid.* 45, 6 (1973).
 [26] N.S. Chant and P.G. Roos, Phys. Rev. C 15, 57 (1977).
 [27] N.S. Chant and P.G. Roos, Phys. Rev. C 27, 1060 (1983).
 [28] P.G. Roos, et al., Phys. Rev. Lett. 40, 1439 (1978).
 [29] A. Nadasen et al., Phys. Rev. C23, 1023 (1981).
 [30] V.G.J. Stoks, R.A.M. Klomp, M.C.M. Rentmeester, and J.J. de Swart, Phys. Rev. C 48, 792 (1993).
 [31] N.S. Chant, P. Kitching, P.G. Roos and L. Antonuk, Phys. Rev. Lett 43, 495 (1979).
 [32] N.Yamaguchi, S. Nagata, and J. Michyama, Prog. Theor. Phys. 70, 459 (1983)
 [33] M.A. Franey and W.G. Love) Phys. Rev. C31, 488 (1985).
 [34] K. Nakayama and W. G. Love, Phys. Rev. C38) 51 (1988).
 [35] J.J. Kelly, Phys. Rev. C 39. 2120 (1989).
 [36] L. Ray: Phys. Rev. C41, 2816 (1990).
 [37] K. Amos, J. Dortmans, H.V. von Geramb, S. Karataglidis and J. Raynal, Adv. Nucl. Phys. 25, 275 (2000).
 [38] C. Horowitz, Phys. Rev. C 31, 1340 (1985).
 [39] E.D. Cooper, S. Harna, B.C. Clark, and R.L. Meecher, Phys. Rev. C 47, 297 (1993).
 [40] P. Kitching, C.A. Miller, W.C. Olsen, D.A. Hutcheon, W.J. McDonald, and A.W. Stetz, Nucl. Phys. A 340, 423 (1980).
 [41] A.N. Antonov et al., Nucl. Instr. Meth. A 637, 60 (2011).
 [42] Toshimi Suda and Haik Simon, “Prospects for electron scattering on unstable, exotic nuclei”, Prog. Part. Nucl. Phys., in press (2017).
 [43] S. Karataglidis, Eur. Phys. J. A 53, 70 (2017).
 [44] I. Tanihata, et al., Phys. Rev. Lett. 55, 2676 (1985).
 [45] S. Abrahamyan, et al., Phys. Rev. Lett. 108, 112502 (2012).
 [46] D.M. Rossi, et al., Phys. Rev. Lett. 111, 242503 (2013).
 [47] A. Trzcinska, et al., Phys. Rev. Lett. 87, 082501 (2001).
 [48] A. Tamii et al., Phys. Rev. Lett. 107, 062502 (2011).
 [49] M. Samyn, S. Goriely, P.-H. Heenen, J.M. Pearson, F. Tondeur, NPA 700, 142 (2002).
 [50] M. Bender, P.-H. Heenen and P.G. Reinhard, Rev. Mod. Phys. 75, 121 (2003).
 [51] C. Bertulani and J. Piekarewicz, “Neutron Star Crust”, Nova Science Publishers, Hauppauge New York (2012)